

A single electron transistor charge sensor in strong rf fields

R. M. Lewis^{1,*}, C. T. Harris^{1,2}, E. A. Shaner¹

¹Sandia National Laboratories, P.O. Box 5800-1423, Albuquerque, NM 87185, USA

²Center for Integrated Nanotechnologies, Sandia National Labs, Albuquerque, NM 87183, USA

We measure the charge sensitivity, S_e , of a single electron transistor (SET) in the presence of strong ($V_{rf} \sim e/C_g$) spurious radio frequency (rf) signals at frequencies up to 50 MHz, where C_g is the gate capacitance. Although S_e appears to degrade when exposed to V_{rf} , we find that broadening of conduction peaks is largely due to the measurement technique and show that S_e is maintained even with strong V_{rf} present. We show cancellation of a known V_{rf} signal at 1 MHz, demonstrating that a stable bias point in the presence of rf signals is possible.

Superconducting single electron transistors (SETs) [1, 2] make exquisite charge sensors due to the sharpness of the conduction resonances between coulomb blockade minima as well as other sharp conduction features. Charge sensitivity of $S_e \approx 1 \times 10^{-5} \text{ electrons}/\sqrt{\text{Hz}}$ or better has been demonstrated in the rf-SET configuration [3, 4]. SETs of various forms have found applications in many areas including sensing the motion of micro-mechanical resonators [5] and as qubit readouts for electrons in Si [6] and GaAs [7] quantum dots. SETs have also been demonstrated as charge counters for electrons on helium films [8]. It is likely that a solid-state spin-based multi-qubit system would use integrated SET charge sensors for readout. In such a system, readout would occur in the presence of crosstalk from neighboring qubits. For example, parallel

* corresponding author, email: rmlawi@sandia.gov

readout of neighboring qubits, gating, clocking, and control logic signals may all be present at varying levels. In this context, we seek to understand how robust is the SET's charge sensitivity and how rapidly the charge sensing performance degrades when rf signals are present.

In this paper, we examine the charge sensing performance of an SET strongly-coupled to spurious radio frequency (rf) signals. Sinusoidal and square waveforms with frequencies f up to 50 MHz were used to simulate control and clock signals in complex quantum circuits. We observe that although small amplitude rf signals ($V_{rf} \ll e/C_g$) broaden the conduction peaks between coulomb blockade minima, this effect is not heating, but rather a *smearing* of the SET conductivity versus gate voltage, V_g , $G_{SET}(V_g)$. Here, e is the electron's charge and C_g is the capacitance of a gate to the SET. Evidence comes from measurements with stronger $V_{rf} \sim e/C_g$ where the conduction peaks split in two and shift outwards in V_g , relative to the original peak, in proportion to the strength of V_{rf} . In these conditions, no additional broadening is seen after the initial splitting when square waveforms are applied and only minimal additional broadening when sinusoidal waveforms are applied. Also, when the rf induced peak shifts add to an integer number of electrons on the SET island, larger conduction peaks are measured due to the overlapping of the shifted peaks and improved charge sensitivity is seen. In a further experiment, we compensated for an applied V_{rf} , producing a stable bias point despite the presence of two rf signals. These results show that a SET can maintain charge sensitivity comparable to $V_{rf} = 0$ even in the presence of relatively large rf signals and extend the application range of the SET.

Our SET was fabricated using double-angle evaporation and in-situ oxidation to create Al/AlOx tunnel junctions [9]. An SEM image of a co-fabricated device, see Fig. 1a, indicates that the junctions are approximately 70 nm by 65 nm in area and have estimated junction capacitance $C_j \approx$

0.23 fF [10]. Each junction has normal resistance $R_n = 450 \text{ k}\Omega$. From R_n and C_j we estimate an intrinsic bandwidth of, $f_{max} = 1/(2\pi R_n C_j) \approx 1.5 \text{ GHz}$ [3].

Conductivity measurements were performed at a temperature of $T \approx 40 \text{ mK}$ in a dilution refrigerator fitted with coaxial wiring and 80 MHz copper powder

filters on all lines. The sample was housed in an aluminum sample box. Standard lock-in technique,

with a small excitation voltage, $V_{ac} = 18 \text{ }\mu\text{V}$ at 83 Hz, was used to measure the current through the SET, I_{ac} , as the gate voltage, V_g , and source-drain bias voltage, V_{sd} , were varied as shown in Fig. 1b.

Room temperature trans-impedance and voltage pre-amplifiers amplified current from the SET.

From this data, we extract the charging energy, $E_c = 87 \text{ }\mu\text{V}$ or about 1 K , and verify the

superconducting gap of aluminum, $\Delta = 193 \text{ }\mu\text{V}$. Also, the coupling of the SET island to the

lithographically defined gate is measured, $C_{g1} = 73 \text{ aF}$. A second gate was created by passing a

bond wire over the chip and SET, so that it has a weak capacitance to the SET island of $C_{g2} \approx 0.5 \text{ aF}$.

Testing the SET's charge sensing performance in the presence of large $V_{rf} \sim e/C_{g2}$ requires good signal to noise and as much dynamic range as possible. Thus, a V_{sd} bias point featuring large

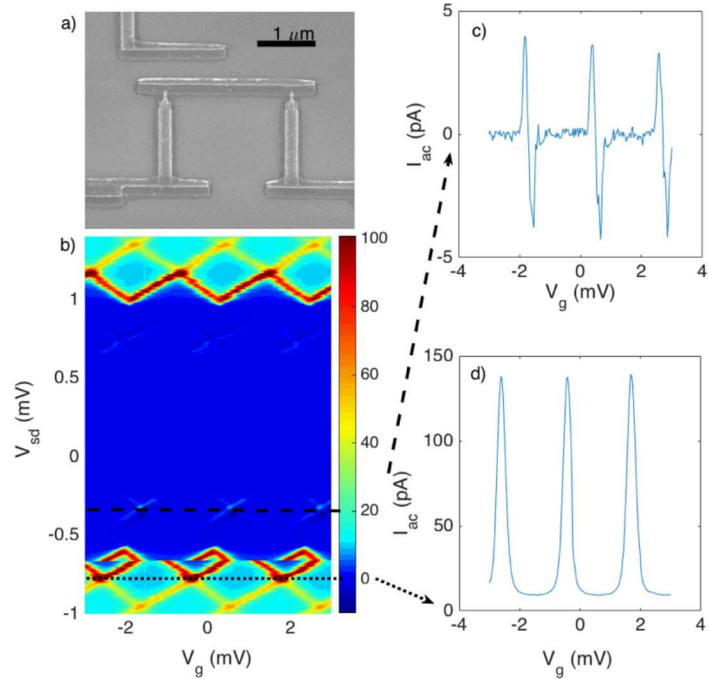


Figure 1. (a) SEM micrograph of the device. (b) Characteristic scan of V_{sd} bias vs. V_g . Line cuts at (c) Josephson quasiparticle resonances and (d) coulomb blockade peaks outside the gap. Note that (b) is unintentionally offset in V_{sd} by about $200 \text{ }\mu\text{V}$, probably by input offsets in the amplifier chain, and a large discontinuity at $V_{sd} = -0.65 \text{ mV}$ is likely due to a range change error in the V_{sd} voltage generator.

conduction peaks is desirable. Inside the superconducting gap, our device shows no conduction except at the Josephson-quasiparticle features [11] where $I_{ac} < 5 \text{ pA}$, shown in Fig. 1c. Although several other good bias points exist, we chose $V_{sd} = -0.775 \text{ mV}$, about $2 E_c$ outside the gap, see Fig. 1d, because it offers the largest conduction peaks and provides excellent signal-to-noise.

Figure 2 shows the results of repeated I_{ac} vs. V_g measurements at $V_{sd} = -0.775 \text{ mV}$ while applying sinusoidal V_{rf} at 1 MHz to the second gate, V_{g2} . The V_{ac} excitation used to measure I_{ac} was

12 μV . The overall pattern of conduction peaks broadening then splitting into two sub-peaks with separation proportionate to the strength of V_{rf} is shown in Fig. 2a. Viewed in real time, V_{rf} would be seen to shift the chemical potential of the SET, μ_{SET} , and hence the conduction peaks, rapidly through a range $\pm V_{rf}/C_{g2}$ many times during the measurement interval—dictated by the time constant of the lock-in amplifier—provided V_{rf} varies slowly

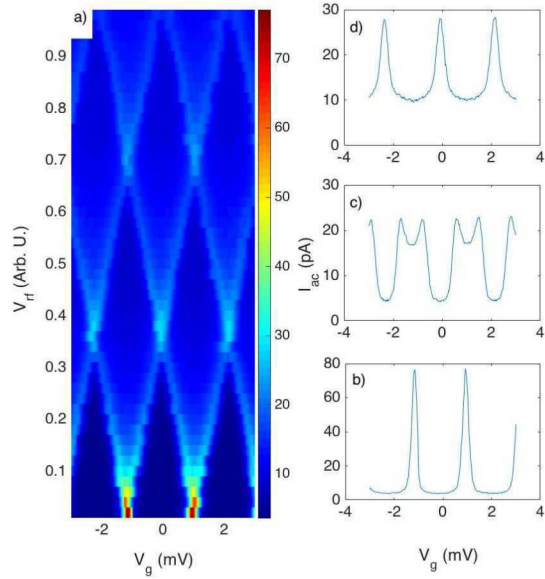


Figure 2. a) Scans of I_{ac} vs V_g with sinusoidal waveform, V_{rf} , at 1 MHz applied. Line cuts at b) $V_{rf} = 0$, c) $V_{rf} = 0.18$, and d) $V_{rf} = 0.33$.

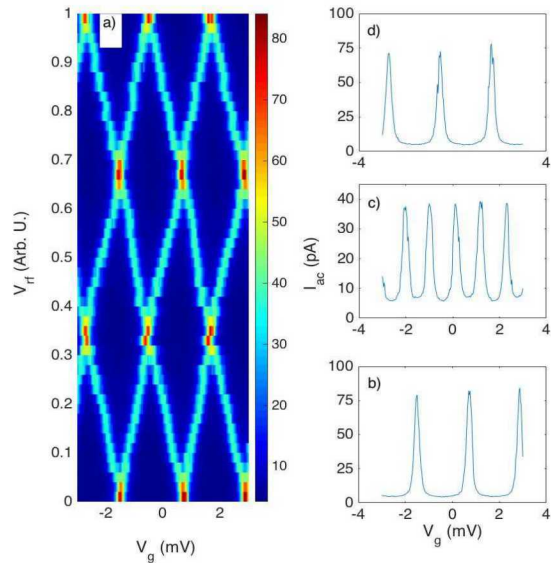


Figure 3. a) Scans of I_{ac} vs. V_g with square waveform at 1 MHz applied (V_{rf}). Line cuts at b) $V_{rf} = 0$, c) $V_{rf} = 0.18$, and d) $V_{rf} = 0.33$.

compared to f_{max} , which is true in these experiments. Because V_{rf} is $\sim 10^4$ times faster than the measurement, I_{ac} vs. V_g in Fig. 2 reflects an average of $G_{SET}(V_g)$. Figure 2b shows I_{ac} vs. V_g with no applied V_{rf} . Small $V_{rf} \ll e/C_{g2}$ blurs this image resulting in broadening of the conduction peaks. Figure 2c was recorded at $V_{rf} = 0.18$, where the conduction peaks have separated into distinct sub-peaks. As V_{rf} increases further, the sub-peaks migrate outwards from the original peak position reflecting that a sinusoidal V_{rf} mostly favors two positions of μ_{SET} . At $V_{rf} = 0.33$, the sub-peak shifts equal $\pm \frac{e}{2}$ and the negative and positive shifted sub-peaks overlap forming a single peak of larger amplitude, shown in Fig. 2d. This scenario repeats at $V_{rf} = 0.66$ where the shift is $\pm e$. A gradual decrease in amplitude of the conduction maxima and increase in conduction elsewhere manifests as the pattern in fig. 2a evolves to higher V_{rf} because the sinewave gives some weight to all possible positions of μ_{SET} between $+V_{rf}$ and $-V_{rf}$. However, even for V_{rf} sufficient to shift the sub-peaks by $\pm \frac{3e}{2}$ strong conduction resonances remain.

A square waveform applied as V_{rf} should result in averaging just two positions of G_{SET} , doubling the measured I_{ac} vs. V_g pattern but producing little or no broadening. Figure 3 shows repeated I_{ac} vs. V_g measurements performed with a square waveform at 1 MHz at the same bias point, $V_{sd} = -0.775$ mV. Figure 3b shows I_{ac} vs. V_g with no applied V_{rf} , and Fig. 3c shows I_{ac} vs. V_g with $V_{rf} = 0.18$, sufficient to split the initial peaks in half and shift them by $\pm \frac{e}{4}$ so that 5 peaks of about ~ 40 pA now appear, half the peak value of I_{ac} seen in Fig. 3b. At $V_{rf} \approx 0.3$, a shift of $\pm \frac{e}{2}$, as in Fig. 3d, three peaks are again seen and of nearly the same amplitude as in Fig. 3b. Overall, a pattern of sub-peaks migrating outward without reduction in fidelity is shown in Fig. 3a, and the topmost line in Fig. 3a, with shifts of $\pm \frac{3e}{2}$, nearly reproduces the lowest line, but with an $\frac{e}{2}$ shift. These observations

support the idea that the SET is responding rapidly to V_{rf} . The absence of broadening at large V_{rf} in Fig. 3a suggests the broadening seen in Fig. 2 was due to I_{ac} averaging the sinusoidal waveform used and not heating caused by the applied MHz frequency of V_{rf} .

The SET charge sensitivity, S_e , is calculated from data in Figs. 2 and 3, taking the measurement bandwidth from the lock-in time constant of 30 ms. The maximum slope, $\Delta I_{ac}/\Delta V_g$ on the side of a conduction peak, is extracted for each I_{ac} vs. V_g measurement, and $S_e = \frac{\delta i}{slope \times V_e \sqrt{BW}}$, is calculated where $\delta i \approx 1$ pA is the current noise in the measurement and $V_e = 2.2$ mV is the change in V_g to add one electron to the SET island. Figure 4 plots S_e vs. V_{rf} for both sine and square waveforms.

Unsurprisingly, the best charge sensitivity was achieved at $V_{rf} = 0$ where $S_e \approx 1.4 \times 10^{-4}$ e/Hz^{1/2}. For sinusoidal waveforms, S_e falls off rapidly as V_{rf} increases. We found a simple functional form, $S_e \sim \alpha V_{rf}^{1/2} + \beta$, the dashed line in Fig. 4, describes this reduction in S_e well; here $\alpha = 2 \cdot 10^{-3}$ and $\beta = 1 \cdot 10^{-4}$. The simplicity of this function roughly allows S_e to be predicted for known

amplitude rf signals. Similar dependence on sinusoidal V_{rf} is seen for frequencies up to 30 MHz as well as at lower frequencies—100 kHz is also shown. In contrast, for square waveforms, S_e vs. V_{rf} remains flat, degrading only by a factor of two relative to $V_{rf} = 0$. Where the split peaks overlap at $V_{rf} \approx 0.33, 0.66,$ and 1 , S_e is nearly as good as at $V_{rf} = 0$.

For square waveforms, S_e at 100 kHz was similar to the 1 MHz data in Fig. 4. In a

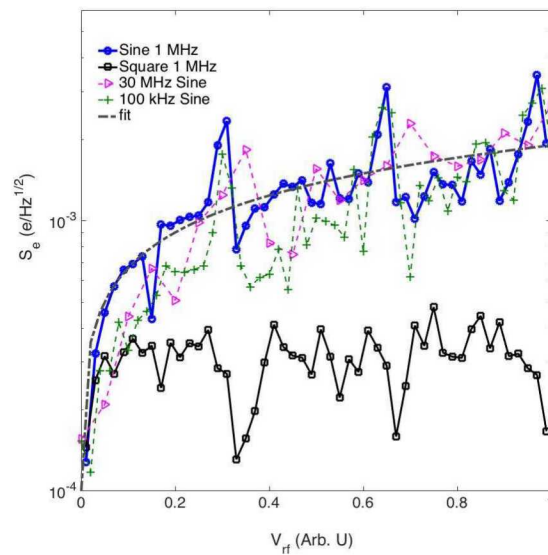


Figure 4. S_e versus V_{rf} for sinusoidal and square waveforms. Data for sinusoidal V_{rf} at 100 kHz and 30 MHz is also shown. The dashed line is a fit to the 1 MHz dataset.

subsequent cool down, we tested V_{rf} of larger amplitudes, up to $\pm 5 e/C_{g2}$, and f up to 50 MHz and saw S_e vs. V_{rf} follow qualitatively similar—flat—results to those shown in Fig. 4, but with worse baseline S_e due to a different V_{sd} bias point.

These data show that charge sensitivity is retained even when large rf signals are applied. To make full use of the potential S_e , a stable bias point is needed, and can be had by applying a compensating signal, V_c , to a gate which nulls V_{rf} . This approach is common in experiments with charge sensors and multiple gates when working at low frequencies or DC.

Figure 5 shows repeated I_{ac} vs. V_g measurements while a compensating signal, V_c , is adjusted to cancel V_{rf} , with traces offset for clarity. In this

measurement, V_g and V_c were applied to the weakly coupled gate, and V_{rf} was applied to the more strongly coupled gate. Although this gate choice was not important to the measurement outcome, it resulted in a broader range of V_g per coulomb blockade peak, and limited how large a signal could be cancelled. Initially, a 1 MHz sine wave of amplitude 0.3 electrons, was applied (dark solid

line) to V_{g2} . V_c was then applied to the gate line, partially cancelling V_{rf} . The amplitude of V_c was gradually increased until full compensation was achieved (dashed red line). A comparison of the gradients along V_g (dI_{ac}/dV_g) of the compensated data (dashed curved) to the uncompensated data (solid curve) shows about a factor of five enhancement in S_e is achieved with compensation. This experiment was performed at 100 kHz and at 1 MHz and is feasible for known interference

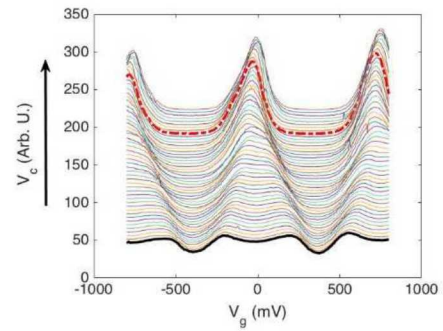


Figure 5. I_{ac} vs. V_g with constant V_{rf} producing $e/3$ splitting. Compensating voltage, V_c , applied with increasing amplitude to remove the splitting.

signals—as phase locking of V_c and V_{rf} is required—up to 50 MHz considering the filtering in our measurement.

In conclusion, we have measured the performance of an SET charge sensor while applying large rf signals to understand how strongly coupled signals affect charge sensitivity. We find the charge sensitivity degrades from $S_e \sim 1.4 \cdot 10^{-4}$ to about, $S_e \sim 4 \cdot 10^{-4}$ when strongly coupled ($V \approx 1 e/C_{g2}$) square waveforms < 50 MHz signals are present or from $S_e \sim 1.4 \cdot 10^{-4}$ to about $S_e \sim 2 \cdot 10^{-3}$ at $V \approx 1 e/C_{g2}$ if sinusoids are used, but that such signals cause little or no heating. Finally, we have demonstrated cancellation of a known spurious signal at 1 MHz indicating that a fixed bias point is possible even in conditions where multiple signals are present as is likely in future quantum processor applications provided these signals are known.

Acknowledgements.

We thank R. J. Schoelkopf and L. Frunzio for advice and a gift of experimental equipment, and J. Aumantado and B. Palmer for helpful discussions. This work was performed, in part, at the Center for Integrated Nanotechnologies, an Office of Science User Facility operated for the U.S. Department of Energy (DOE) Office of Science. Sandia National Laboratories is a multi-mission laboratory managed and operated by National Technology and Engineering Solutions of Sandia, LLC, a wholly owned subsidiary of Honeywell International, Inc., for the U.S. Department of Energy's National Nuclear Security Administration under contract DE-NA0003525. This paper describes objective technical results and analysis. Any subjective views or opinions that might be expressed in the paper do not necessarily represent the views of the U.S. Department of Energy or the United States Government.

References:

- [1] D. V. Averin and K. K. Likharev, *J. Low Temp. Phys.* **62**, pp. 345-373 (1986).
- [2] T. A. Fulton and G. J. Dolan, 'Observation of single-electron charging effects in small tunnel junctions', *Phys. Rev. Lett.* **59**, 109, (1987).
- [3] R. J. Schoelkopf, P. Wahlgren, A. A. Kozhevnikov, P. Delsing, and D. E. Prober, 'The Radio-Frequency Single-Electron Transistor (RF-SET): A Fast and Ultrasensitive Electrometer', *Science* **280**, 1238, (1998).
- [4] A. Aassime, D. Gunnarsson, K. Bladh, and P. Delsing, and R. J. Schoelkopf, 'Radio-frequency single-electron transistor: Toward the shot-noise limit', *Appl. Phys. Lett.* **79**, 4031 (2001).
- [5] M. D. LaHaye, O. Buu, B. Camarota, K. C. Schwab, 'Approaching the quantum limit of a nanomechanical resonator', *Science*, **304** (5667):74-7 (2004).
- [6] A. Morello et al., 'single-shot readout of an electron spin in silicon', *Nature* **467**, 687 (2010).
- [7] W. Lu, A. J. Rimberg, K. D. Maranowski, and A. C. Gossard, 'Single-electron transistor strongly coupled to an electrostatically defined quantum dot', *Appl. Phys. Lett.* **77**, 2746 (2000); doi: 10.1063/1.1320455.
- [8] G. Papageorgiou, P. Glasson, K. Harrabi, V. Antonov, E. Collin, P. Fozooni, P. G. Frayne, M. J. Lea, and D. G. Rees, and Y. Mukharsky, 'Counting Individual Trapped Electrons on Liquid Helium', *Appl. Phys. Lett.* **86**, 153106 (2005).
- [9] G. J. Dolan, 'Offset masks for lift-off processing', *Appl. Phys. Lett.* **31**, 337 (1977); doi: 10.1063/1.89690.
- [10] We assumed a specific capacitance of $50 \text{ fF } \mu\text{m}^{-2}$.
- [11] P. Hadley, E. Delvigne, E. H. Visscher, S. Lahteenmaki, and J. E. Mooij, '3e tunneling processes in a superconducting single-electron tunneling transistor', *Phys. Rev. B* **58**, 15317 (1998).